Available online at www.sciencedirect.com
ScienceDirect
Mathematics and Computers in Simulation 178 (2020) 625–645
MATHEMATICS AND COMPUTERS IN SIMULATION
www.elsevier.com/locate/matcom

Original articles

Stability analysis of a fractional online social network model

John R. Graef[a], Lingju Kong[a,*], Andrew Ledoan[a], Min Wang[b]

[a] Department of Mathematics, University of Tennessee at Chattanooga, Chattanooga, TN 37403, USA
[b] Department of Mathematics, Kennesaw State University, Marietta, GA 30060, USA

Received 16 September 2019; received in revised form 1 July 2020; accepted 12 July 2020
Available online 18 July 2020

Abstract

By drawing an analogy to the spreading dynamics of an infectious disease, the authors derive a fractional-order susceptible–infected–removed (SIR) model to examine the user adoption and abandonment of online social networks, where adoption is analogous to infection, and abandonment is analogous to recovery. They modify the traditional SIR model with demography, so that both infectious and noninfectious abandonment dynamics are incorporated into the model. More precisely, they consider two types of abandonment: (i) infectious abandonment resulting from interactions between an abandoned and an adopted member, and (ii) noninfectious abandonment which is not influenced by an abandoned member. In addition, they study the existence and uniqueness of nonnegative solutions of the model, as well as the existence and stability of its equilibria. They establish a nonnegative threshold quantity R_0^α for the model and show that if $R_0^\alpha < 1$, the user-free equilibrium E_0 is locally asymptotically stable. In addition, they find a region of attraction for E_0. If $R_0^\alpha > 1$, they prove that the model has a unique user-prevailing equilibrium E^* that is globally asymptotically stable. Their stability results also show that the infectious abandonment dynamics do not contribute to the stability of the user-free and user-prevailing equilibria, and that it only affects the location of the user-prevailing equilibrium. The Jacobian matrix technique and the Lyapunov function method are used to show the stability of the equilibria. They perform numerical simulations to verify these theoretical results. Finally, they conduct a case study of fitting their model to some historical Instagram user data to show the effectiveness of the model.

Keywords: Online social networks; Fractional-order SIR models; Equilibrium; Stability analysis; Lyapunov functions; Numerical simulation

1. Introduction

In recent years online social networks (OSNs) have become more prevalent in the diffusion of information and the building of social relations among a huge number of people. With OSNs, information on the latest news headlines, election results, etc., can be effectively spread across vast networks. This process is referred to as information diffusion [50]. Because OSNs have a significant impact on society [20,22], it has become increasingly important to gain a deeper understanding of their dynamics. As a result, this may increase the efficiency of distributing relevant information to any given user and reduce unwanted information over social media. Thus, a variety of techniques and methods have been developed by numerous researchers to understand network structure, user interactions, traffic

* Corresponding author.
E-mail addresses: John-Graef@utc.edu (J.R. Graef), Lingju-Kong@utc.edu (L. Kong), Andrew-Ledoan@utc.edu (A. Ledoan), mwang23@kennesaw.edu (M. Wang).

https://doi.org/10.1016/j.matcom.2020.07.012
0378-4754/

properties [6,8,26,39,46], and to investigate the characteristics of information diffusion [31,47]. These mentioned works employ empirical approaches, utilizing data mining and statistical schemes, to study the characteristics of information diffusion over OSNs. However, it is still a difficult task to fully understand information diffusion over OSNs due to the intricacy of human dynamics and social interactions, the rapid change of social network platforms, and the large scale of users and information [9,50].

Recently, mathematical modeling has played an increasing role in understanding information diffusion in OSNs since they can predict how a specific diffusion process would unfold in a given network from the temporal process and/or spatial point of view by learning from past diffusion processes [8,9,30,36,50]. Modeling how information spreads is of outstanding interest for stopping the spread of viruses, analyzing how misinformation spreads, etc [20]. Most models can be classified as either graph based predictive models or non-graph based predictive models [20]. In the present paper, we study non-graph based predictive models. Partial differential equation (PDE) models and epidemiological models based on ordinary differential equations (ODEs) are two important non-graph based predictive models. The former models are built on the intuitive cyber-distance among online users and can be used to study both temporal and spatial patterns of information diffusion processes in OSNs. The dynamics of these models is given by a logistic equation that models the density of influenced users at a given distance from the source and at a given time. Some recent work on such models include [9,30,50]. The latter models only consider temporal process and can be used to describe user adoption and abandonment dynamics of user activity of OSNs. With large amounts of data available to researchers, it can also be used to predict the future trend of a given online platform. Some known work on models based on ODEs can be found in [23,32,35,36,49,52]. In particular, papers [35,36] used ODE compartmental models to study the dynamical behaviors of rumor spreading in complex social networks with hesitating mechanisms. Paper [23] established an interplay ODE model with impulsive effects between official information and rumor spreading to stimulate government emergency strategies. In [49], the authors proposed an ODE information spreading model including the mechanisms of sharing, reviewing, collecting, and stifling to describe the dynamic process of information spreading.

We would like to point out that most existing results on OSNs study how information spreads in OSNs. Work on user adoption and abandonment of OSNs can be rarely seen in the literature. To the best of our knowledge, the only paper studying user adoption and abandonment of OSNs is the paper [8] where a modified epidemiological model was used to explain user adoption and abandonment of OSNs (see Eq. (3.1) in Section 3 for the model). Our goal in this paper is to study the user adoption and abandonment of an OSN. Thus, this work will fill the research void on this subject.

Moreover, our search of the literature shows that all the available mathematical models for OSNs currently utilize derivatives and integrals of integer order. As it is noted in [28], the classical calculus provides a powerful tool for explaining and modeling important dynamic processes in many areas of applied sciences. However, many complex systems have anomalies such as network traffic and cellular diffusion processes, to name a few. The dynamics of these processes cannot be fully characterized by classic derivative models. Fractional differential equations are more useful here because of their nonlocal nature; that is, they possess memory and can capture the history of the variables. Another advantage of fractional-order systems is that greater degrees of freedom are allowed in the models. For instance, in [12] a better approximation to the known real data is obtained for a dengue fever outbreak model of fractional-order by adjusting the values of the order. The reader is referred to [4,11,12,17,28,34,43] for more details on the benefits of models based on fractional differential equations. In recent years fractional differential equations have become more popular, as they have been applied to many different types of dynamical systems. See [2–4,10–12,19,21,24,25,37,42] and the references therein for recent works.

In this paper we will first construct a fractional-order epidemiological model to study user adoption and abandonment of an OSN, with adoption being analogous to infection and abandonment being analogous to recovery. Our model utilizes fractional-order ODEs and modifies the traditional susceptible–infected–removed (SIR) model with demography, so that it incorporates both infectious and noninfectious abandonment dynamics; i.e., the infectious abandonment as a result of interactions between abandoned and adopted members and the noninfectious abandonment without being influenced by abandoned members. We then discuss the existence and uniqueness of nonnegative solutions of the model and study the existence and stability of its equilibria. We utilize the Jacobian matrix technique and the Lyapunov function method to show the stability of the equilibria. We perform numerical simulations to illustrate our results. Finally, we demonstrate the performance of our model by fitting it to some historical Instagram user data.

We want to comment that our model (see Eq. (3.9)) covers the integer-order model as a special case. Please refer to the last paragraph in Section 3 for a discussion on this. Even for the integer-order case, the model is still new and was not previously studied in the literature.

The rest of this paper is organized as follows: Section 2 contains some preliminary results, Section 3 studies the model formulation, Section 4 discusses the existence and uniqueness of nonnegative solutions of the model, Section 5 investigates the equilibria and stability analysis of the model, Section 6 presents numerical simulations of the theoretical results, Section 7 contains a case study of fitting our model to some historical Instagram data, and finally, Section 8 summarizes the conclusions of the paper.

2. Preliminary results

We first recall some basic definitions and properties of the fractional calculus. Additional information on fractional calculus can be found in [11,28,43].

Definition 2.1. Let f be a function defined on $[a,b]$ and $\eta > 0$. The Riemann–Liouville fractional integral of order η for the function f is defined by

$$ {}_aD_t^{-\eta} f(t) = \frac{1}{\Gamma(\eta)} \int_a^t (t-s)^{\eta-1} f(s) ds, \quad t \in [a,b], $$

provided the right-hand side is pointwise defined on $[a,b]$, where $\Gamma(\cdot)$ is the gamma function. For $\eta = 0$, we set ${}_aD_t^0 = I$, the identity operator.

Remark 2.1. When $\eta = n \in \mathbb{N}$, ${}_aD_t^{-\eta} f(t)$ coincides with the nth integral of the form

$$ {}_aD_t^{-n} f(t) = \frac{1}{(n-1)!} \int_a^t (t-s)^{n-1} f(s) ds, \quad t \in [a,b]. $$

Let $AC([a,b],\mathbb{R})$ be the space of real-valued functions f that are absolutely continuous on $[a,b]$. For $n \in \mathbb{N}$, let $AC^n([a,b],\mathbb{R})$ be the space of real-valued functions f that have continuous derivatives up to order $n-1$ on $[a,b]$ such that $f^{(n-1)} \in AC([a,b],\mathbb{R})$.

Definition 2.2. Let $\eta \geq 0$, $n \in \mathbb{N}$, and $f \in AC^n([a,b],\mathbb{R})$. The Caputo fractional derivative of order η for the function f is defined by

$$ {}_a^CD_t^{\eta} f(t) = \begin{cases} {}_aD_t^{-(n-\eta)} f^{(n)}(t) = \dfrac{1}{\Gamma(n-\eta)} \displaystyle\int_a^t (t-s)^{n-\eta-1} f^{(n)}(s) ds, & n-1 < \eta < n, \\ f^{(n)}(t), & \eta = n. \end{cases} $$

It is known that ${}_a^CD_t^{\eta} f(t) \to f^{(n-1)}(t) - f^{(n-1)}(0)$ as $\eta \to n-1$ and ${}_a^CD_t^{\eta} f(t) \to f^{(n)}(t)$ as $\eta \to n$.

Definition 2.3. Let $\eta > 0$. The function E_η defined by

$$ E_\eta(z) = \sum_{j=0}^{\infty} \frac{z^j}{\Gamma(j\eta + 1)} $$

is called the Mittag-Leffler function of order η.

The function $E_\eta(z)$ is entire. For the special cases where $\eta = 1$ and $\eta = 2$, we have

$$ E_1(z) = e^z \quad \text{and} \quad E_2(z) = \cosh(\sqrt{z}). $$

Lemma 2.1 ([11]). *If f is continuous and $\eta \geq 0$, then ${}_a^CD_t^{\eta}\, {}_aD_t^{-\eta} f(t) = f(t)$.*

Lemma 2.2 ([11]). *If $\eta > 0$, $r > 0$, $\varphi \in [-\pi,\pi]$, and $\lambda = re^{i\varphi}$, then $\lim_{t\to\infty} E_\eta(-\lambda t^\eta) = 0$ for $|\varphi| < \frac{\eta\pi}{2}$.*

We now present some results related to the stability of fractional-order systems. Let Ω be an open subset of $\mathbb{R}^n$. For $\alpha \in (0, 1]$, we consider the initial value problem (IVP) consisting of an autonomous fractional-order system

$$ {}_a^C D_t^\alpha x(t) = g(x), \quad x(t_0) = x_0, \tag{2.1}$$

where $g : \Omega \to \mathbb{R}^n$ is locally Lipschitz continuous in x.

Definition 2.4. A point x^* is called an equilibrium of the system (2.1) if $g(x^*) = 0$.

Lemma 2.3 (*[3,19,41]*). *Let $J(x^*)$ denote the Jacobian matrix of the system (2.1) evaluated at an equilibrium point x^*, and let λ_i, $i = 1, \ldots, n$, be the eigenvalues of $J(x^*)$. Then x^* is locally asymptotically stable if and only if $|\arg(\lambda_i)| > \frac{\alpha\pi}{2}$, $i = 1, \ldots, n$.*

To prove our stability results, we will use the following lemma, whose parts (a) and (b) are proved in [1, Lemma 1] and [48, Lemma 3.1], respectively.

Lemma 2.4. *Assume that $\alpha \in (0, 1]$ and $f \in AC([a, \infty), \mathbb{R}^+)$. For any $t \geq a$, we have*

(a) $\frac{1}{2}{}_a^C D_t^\alpha f^2(t) \leq f(t){}_a^C D_t^\alpha f(t)$;
(b) ${}_a^C D_t^\alpha \left[f(t) - f^* - f^* \ln \frac{f(t)}{f^*} \right] \leq \left(1 - \frac{f^*}{f(t)}\right) {}_a^C D_t^\alpha f(t)$, where $f^* \in \mathbb{R}^+$.

Let $V \in C^1(\Omega, \mathbb{R})$ and $\alpha \in (0, 1]$. The αth order Caputo derivative of $V(x)$ along the solution $x(t)$ of the system ${}_a^C D_t^\alpha x(t) = g(x)$, $t \in [a, \infty)$, is given by

$$ {}_a^C D_t^\alpha V(x(t)) = {}_a D_t^{-(1-\alpha)} \left(\frac{dV}{dx} \frac{dx}{dt} \right). $$

We will also need the following fractional version of the well-known LaSalle's invariance principle.

Lemma 2.5 (*[24]*). *Assume that $\mathcal{D}$ is a bounded closed set in $\mathbb{R}^n$ and that every solution of ${}_a^C D_t^\alpha x(t) = g(x)$, $t \in [a, \infty)$, starting from a point in $\mathcal{D}$, remains in $\mathcal{D}$ for all time t. Assume, further, that $V \in C^1(\mathcal{D}, \mathbb{R})$ such that ${}_a^C D_t^\alpha V(x(t)) \leq 0$, where $x(t)$ is any solution of the system ${}_a^C D_t^\alpha x(t) = g(x)$. Let $E = \{x \in \mathcal{D} : {}_a^C D_t^\alpha V = 0\}$, and let M be the largest invariant subset of E. Then every solution $x(t)$ of ${}_a^C D_t^\alpha x(t) = g(x)$, $t \in [a, \infty)$, originating in $\mathcal{D}$ tends to M as $t \to \infty$. In particular, if $M = \{0\}$, $x(t) \to 0$ as $t \to \infty$.*

3. Model formulation

3.1. An integer order SIR model

Many epidemiological models have been developed to better understand the transmission pattern of infectious diseases [38]. A simple and well-studied model, introduced by Kermack and McKendrick in [27], is the SIR model. In this model, derivatives of integer order are utilized and the entire population N is divided into three compartments or classes: susceptible (S), infected (I), and recovered/immune (R). The flows of people between the three compartments are modeled. The applications of epidemiological models to non-disease situations have been previously proposed in [5,7,8,51] to model the spread of less tangible notions such as ideas. In [8] the authors remarked that ideas, akin to disease, spread infectiously between people before eventually dying out. Communicative contacts between different people spread ideas. People ultimately lose interest in the idea and no longer manifest it, which can be regarded as the gain of immunity to the idea. By drawing an analogy to the dynamics that govern the spread of an infectious disease, the authors propose the infectious recovery SIR model

$$ \begin{cases} S' = -\dfrac{\delta I S}{N}, \\ I' = \dfrac{\delta I S}{N} - \dfrac{\eta I_1 R}{N}, \\ R' = \dfrac{\eta I R}{N}, \end{cases} \tag{3.1}$$

Table 1
Descriptions of the model parameters.

Notations	Meaning	Units
S	Potential OSN new users	Number of people
I	OSN current users	Number of people
R	Population opposed to OSN use	Number of people
N	The summation of S, I, and R	Number of people
A	Recruitment/migration rate of new users into the population	Number of people per unit of time
δ	Transmission rate at which potential users join OSN	[Number of people $\times$unit of time]$^{-1}$
η	OSN infectious abandonment rate as a result of interactions with people who opposed to OSN use	[Number of people $\times$unit of time]$^{-1}$
μ	Per capita natural death rate	[Unit of time]$^{-1}$
ν	OSN noninfectious abandonment rate without being influenced by other users who opposed to OSN use	[Unit of time]$^{-1}$

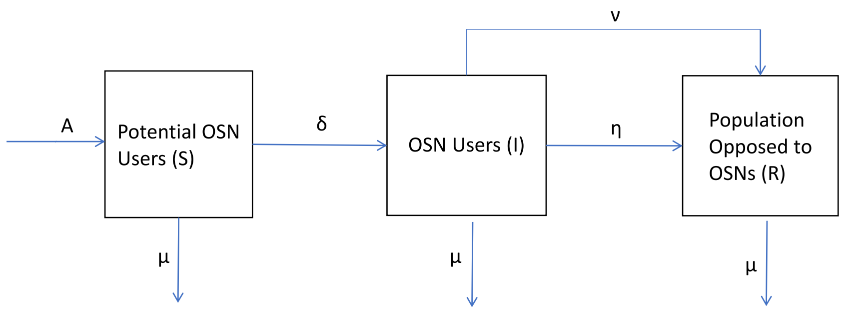

Fig. 1. Conceptual illustration of the OSN dynamics in the model (3.2).

to analyze user adoption and abandonment of OSNs, where, as noted above, adoption is analogous to infection and abandonment is analogous to recovery. The OSN dynamical interpretation of the parameters in the model (3.1) can be found in Table 1.

The model (3.1) utilizes the standard incidence and assumes that the total population is a constant and that contact between a recovered and an infected member of the population is required for recovery. However, in practice the number of total users may not be a constant as a result of population migration or death. Users may quit OSNs because of other reasons without being influenced by recovered users. The contacts among users may increase with an increase in the total population. To incorporate these considerations, the modified version of the traditional SIR model with demography

$$\begin{cases} S' = A - \delta SI - \mu S, \\ I' = \delta SI - \eta IR - (\mu + \nu)I, \\ R' = \eta IR + \nu I - \mu R, \end{cases} \tag{3.2}$$

can be used, where the mass action incidence is utilized. The descriptions of the model parameters are provided in Table 1. Here two kinds of abandonment dynamics are considered in the model (3.2). Its flowchart is shown in Fig. 1.

For models (3.1) and (3.2), the state at each time does not depend on the previous history of the systems. They are memoryless, so-called Markovian, processes. However, the epidemic processes evolution and control in human societies cannot be considered without any memory effect. When an idea spreads within a human population, the experience or knowledge of individuals about that idea should affect their responses. As noted above, fractional differential equations are valuable tools to model the dynamics of OSNs. It has been observed in [4,11,12,17] that models based on fractional-order derivatives can provide better agreement between measured and simulated data than classical models based on integer order derivatives.

3.2. A fractional-order SIR model

We wish to convert the model (3.2) into a fractional-order problem that will incorporate memory effects into the system. One way to approach this might seem to be to just replace the derivatives on the left hand sides of the equations in the system (3.2) by the corresponding Caputo fractional derivatives. This results in the model

$$\begin{cases} {}_0^C D_t^\alpha S = \Lambda - \delta S I - \mu S, \\ {}_0^C D_t^\alpha I = \delta S I - \eta I R - (\mu + \nu) I, \\ {}_0^C D_t^\alpha R = \eta I R + \nu I - \mu R. \end{cases} \tag{3.3}$$

However, this model is not consistent. A simple dimensional analysis shows that the expressions on the left hand of (3.3) have the dimension of $(\text{time})^{-\alpha}$, and all right hand sides of (3.3) have the dimension of $(\text{time})^{-1}$. Such flaws have been observed in the papers [12,15,45]. These papers also discussed how to fix the dimension mismatch; see [12, p. 616] [1], [15, p. 204], and [45, pp. 513–515].

To construct a dimensionally consistent model, we assume that the initial populations of the three compartments satisfy the initial conditions (ICs)

$$S(0) = S_0, \quad I(0) = I_0, \quad \text{and} \quad R(0) = R_0, \tag{3.4}$$

where S_0, I_0, and R_0 are nonnegative real numbers. The model (3.2) is equivalent to the integral form

$$\begin{cases} S(t) = S_0 + \int_0^t [\Lambda - \delta S(s) I(s) - \mu S(s)]\, ds, \\ I(t) = I_0 + \int_0^t [\delta S(s) I(s) - \eta I(s) R(s) - (\mu + \nu) I(s)]\, ds, \\ R(t) = R_0 + \int_0^t [\eta I(s) R(s) + \nu I(s) - \mu R(s)]\, ds. \end{cases} \tag{3.5}$$

In order to include the influence of memory effects, we rewrite (3.5) in terms of time-dependent integrals

$$\begin{cases} S(t) = S_0 + \int_0^t M(t,s) [\Lambda - \delta S(s) I(s) - \mu S(s)]\, ds, \\ I(t) = I_0 + \int_0^t M(t,s) [\delta S(s) I(s) - \eta I(s) R(s) - (\mu + \nu) I(s)]\, ds, \\ R(t) = R_0 + \int_0^t M(t,s) [\eta I(s) R(s) + \nu I(s) - \mu R(s)]\, ds, \end{cases} \tag{3.6}$$

where $M(t,s)$ plays the role of a time-dependent memory kernel and is equal to a delta function $\delta(t,s)$ in a classical Markov process. To incorporate long-term memory effects, a proper choice of M can be a power-law correlation function [2,44] which exhibits a slow decay such that the state of the system at early times also contributes to the evolution of the system. Thus, we select

$$M(t,s) = \frac{1}{\Gamma(\alpha)} (t-s)^{\alpha-1}, \quad \alpha \in (0,1].$$

Substituting this choice for M into (3.6) and using Definition 2.1, we obtain

$$\begin{cases} S(t) - S_0 = {}_0 D_t^{-\alpha} [\Lambda - \delta S(t) I(t) - \mu S(t)], \\ I(t) - I_0 = {}_0 D_t^{-\alpha} [\delta S(t) I(t) - \eta I(t) R(t) - (\mu + \nu) I(t)], \\ R(t) - R_0 = {}_0 D_t^{-\alpha} [\eta I(t) R(t) + \nu I(t) - \mu R(t)]. \end{cases} \tag{3.7}$$

Once again, the dimensions of the system (3.7) are technically somewhat inconsistent. For each equation, the left hand side has the dimension of number of people, and the right hand side has the dimension of number of people $\times$ $[\text{unit of time}]^{\alpha-1}$. Thus, we need to modify the right-hand sides to make the dimensions match. One straightforward way of doing this is to write (3.7) as follows:

$$\begin{cases} S(t) - S_0 = {}_0 D_t^{-\alpha} [\Lambda^\alpha - \beta^\alpha S(t) I(t) - \mu^\alpha S(t)], \\ I(t) - I_0 = {}_0 D_t^{-\alpha} [\beta^\alpha S(t) I(t) - \gamma^\alpha I(t) R(t) - (\mu^\alpha + \nu^\alpha) I(t)], \\ R(t) - R_0 = {}_0 D_t^{-\alpha} [\gamma^\alpha I(t) R(t) + \nu^\alpha I(t) - \mu^\alpha R(t)], \end{cases} \tag{3.8}$$

where μ and ν are given in Table 1 and the dynamical interpretation of Λ, β, and γ is given in Table 2.

Table 2
Dynamical interpretation of Λ, β, and γ.

Notations	Meaning	Units
Λ	Recruitment/migration rate of new users into the population	[Number of people]$^{\frac{1}{\alpha}}$ $\times$[unit of time]$^{-1}$
β	Transmission rate at which potential users join OSN	[Number of people]$^{-\frac{1}{\alpha}}$ $\times$[unit of time]$^{-\alpha}$
γ	OSN infectious abandonment rate as a result of interactions with people who opposed to OSN use	[Number of people]$^{-\frac{1}{\alpha}}$ $\times$[unit of time]$^{-\alpha}$

Now, applying a fractional Caputo derivative of order α on both sides of each equation in (3.8) and Lemma 2.1, we derive the fractional-order model

$$\begin{cases} {}_0^C D_t^\alpha S = \Lambda^\alpha - \beta^\alpha SI - \mu^\alpha S, \\ {}_0^C D_t^\alpha I = \beta^\alpha SI - \gamma^\alpha IR - (\mu^\alpha + \nu^\alpha)I, \\ {}_0^C D_t^\alpha R = \gamma^\alpha IR + \nu^\alpha I - \mu^\alpha R. \end{cases} \tag{3.9}$$

Both sides of the equations in (3.9) have the same dimensions. Here and henceforth, we focus our attention on this model.

When introducing a convolution integral with a power-law memory kernel, fractional derivatives are useful to describe memory effects in the dynamics of OSNs. The decaying rate of the memory kernel M depends on the value of α. A smaller value of α corresponds to more slowly decaying time-correlation functions. In [17] a justification of the fractional-order derivative is given, and it is shown that the fractional order α can be interpreted as an index of memory of the system. Since ${}_0^C D_t^\alpha y(t) \to y'(t)$ as $\alpha \to 1^-$, the model (3.9) tends toward the memoryless model (3.2) as $\alpha \to 1$. Thus, the model (3.2) can be regarded as a special case of the model (3.9). For simplicity, the same memory contributions (i.e., the same value of α) are assumed in the model (3.2) for different states of S, I, and R. When having different memory contributions, the technique introduced in [16] can be employed to obtain a fractionalization of the model (3.2). More complicated kernel functions could be investigated to take into account different time scales. Related ideas on fractionalization of integer order models can be found in [15,16,37,44].

4. Existence and uniqueness of nonnegative solutions

We begin with an existence and invariance result for our model.

Theorem 4.1. *The model (3.9), with the ICs (3.4), has a unique nonnegative solution for every* $(S_0, I_0, R_0) \in \mathbb{R}_+^3$. *Moreover, the compact set*

$$\Omega = \left\{ (S, I, R) \in \mathbb{R}_+^3 \ : \ 0 \le S + I + R \le \frac{\Lambda^\alpha}{\mu^\alpha} \right\} \tag{4.1}$$

is a positively invariant set and attracts all solutions of the model (3.9) initiating in $\mathbb{R}_+^3$.

Proof. Let

$$X(t) = \begin{pmatrix} S(t) \\ I(t) \\ R(t) \end{pmatrix}, \quad X_0 = \begin{pmatrix} S_0 \\ I_0 \\ R_0 \end{pmatrix},$$

and

$$f(X(t)) = \begin{pmatrix} f_1(X(t)) \\ f_2(X(t)) \\ f_3(X(t)) \end{pmatrix} = \begin{pmatrix} \Lambda^\alpha - \beta^\alpha SI - \mu^\alpha S \\ \beta^\alpha SI - \gamma^\alpha IR - (\mu^\alpha + \nu^\alpha)I \\ \gamma^\alpha IR + \nu^\alpha I - \mu^\alpha R \end{pmatrix}.$$

The model (3.9), with the ICs (3.4), can be written as ${}_0^C D_t^\alpha X = f(X)$ with $X(0) = X_0$. The Jacobian matrix $\frac{\partial f}{\partial X} = \frac{\partial(f_1, f_2, f_3)}{\partial(S, I, R)}$ of f is continuous on $\mathbb{R}_+^3$. By [29, Remark 1.2.1], f is locally Lipschitz on $\mathbb{R}_+^3$. By [33, Remark 3.8], the model (3.9), with the ICs (3.4), has a unique solution for every $(S_0, I_0, R_0) \in \mathbb{R}_+^3$.

We show that, for every $(S_0, I_0, R_0) \in \mathbb{R}_+^3$, the unique solution (S, I, R) of model (3.9), with the ICs (3.4), is nonnegative. We deny and distinguish seven cases.

Case (a): There exist $t_S, t_I, t_R \in (0, \infty)$ such that

$$S(t_S) < 0 \text{ and } S(t) \geq 0 \quad \text{for all } t \in [0, t_S), \tag{4.2}$$

$$I(t_I) < 0 \text{ and } I(t) \geq 0 \quad \text{for all } t \in [0, t_I), \tag{4.3}$$

$$R(t_R) < 0 \text{ and } R(t) \geq 0 \quad \text{for all } t \in [0, t_R). \tag{4.4}$$

Case (b): $S(t)$ is nonnegative on $\mathbb{R}_+$, and (4.3) and (4.4) hold.
Case (c): $I(t)$ is nonnegative on $\mathbb{R}_+$, and (4.2) and (4.4) hold.
Case (d): $R(t)$ is nonnegative on $\mathbb{R}_+$, and (4.2) and (4.3) hold.
Case (e): $S(t), I(t)$ are nonnegative on $\mathbb{R}_+$ and (4.4) holds.
Case (f): $S(t), R(t)$ are nonnegative on $\mathbb{R}_+$ and (4.3) holds.
Case (g): $I(t), R(t)$ are nonnegative on $\mathbb{R}_+$ and (4.2) holds.

Below, we prove by contradiction that none of these cases can occur. Assume that Case (a) holds. There are three possibilities here.

Subcase (a1): $t_S = \min\{t_S, t_I, t_R\}$. From the first equation in (3.9),

$${}_0^C D_t^\alpha S \geq -(\beta^\alpha I + \mu^\alpha) S \geq -\kappa_1 S,$$

where $\kappa_1 = \beta^\alpha \max_{t \in [0, t_S]} I(t) + \mu^\alpha > 0$. Thus,

$$S(t) \geq S(0) E_\alpha(-\kappa_1 t^\alpha) \quad \text{for all } t \in [0, t_S].$$

Hence, $S(t_S) \geq 0$. This contradicts the assumption that $S(t_S) < 0$.

Subcase (a2): $t_I = \min\{t_S, t_I, t_R\}$. From the second equation in (3.9),

$${}_0^C D_t^\alpha I \geq -(\gamma^\alpha R + \mu^\alpha + \nu^\alpha) I \geq -\kappa_2 I,$$

where $\kappa_2 = \gamma^\alpha \max_{t \in [0, t_I]} R(t) + \mu^\alpha + \nu^\alpha > 0$. Thus,

$$I(t) \geq I(0) E_\alpha(-\kappa_2 t^\alpha) \quad \text{for all } t \in [0, t_I].$$

Hence, $I(t_I) \geq 0$. This contradicts the assumption that $I(t_I) < 0$.

Subcase (a3): $t_R = \min\{t_S, t_I, t_R\}$. From the third equation in (3.9),

$${}_0^C D_t^\alpha R \geq -\mu^\alpha R \quad \text{for all } t \in [0, t_R].$$

Thus,

$$R(t) \geq R(0) E_\alpha(-\mu^\alpha t^\alpha) \quad \text{for all } t \in [0, t_R].$$

Hence, $R(t_R) \geq 0$. This contradicts the assumption $R(t_R) < 0$.

Combining Subcases (a1)–(a3), we conclude that Case (a) cannot occur.

Assume now that Case (b) holds. Proceeding similarly as in Case (a) and considering the subcases $t_I = \min\{t_I, t_R\}$ and $t_R = \min\{t_I, t_R\}$, we can show that Case (b) cannot occur either. Similar arguments can be used to show that Cases (c)–(g) cannot occur. Since none of Cases (a)–(g) can occur, we conclude that the unique solution (S, I, R) is nonnegative.

Next, we prove that the set Ω, defined by (4.1), is positively invariant. By adding the equations in (3.9), we obtain

$${}_0^C D_t^\alpha (S + I + R) = \Lambda^\alpha - \mu^\alpha (S + I + R);$$

i.e.,

$${}_0^C D_t^\alpha N = \Lambda^\alpha - \mu^\alpha N.$$

In view of [11, Remark 7.1] (or [28, Proposition 5.10]), it follows that

$$\begin{aligned} N(t) &= N(0) E_\alpha(-\mu^\alpha t^\alpha) + \Lambda^\alpha \alpha \int_0^t s^{\alpha-1} E'_\alpha(-\mu^\alpha t^\alpha) ds \\ &= \left(-\frac{\Lambda^\alpha}{\mu^\alpha} + N(0)\right) E_\alpha(-\mu^\alpha t^\alpha) + \frac{\Lambda^\alpha}{\mu^\alpha}. \end{aligned} \tag{4.5}$$

Here we note that $E_\alpha(-\mu^\alpha t^\alpha) \geq 0$. If $N(0) \leq \frac{\Lambda^\alpha}{\mu^\alpha}$, we have

$$S(t) + I(t) + R(t) = N(t) \leq \frac{\Lambda^\alpha}{\mu^\alpha}.$$

Thus, Ω is positively invariant.

Finally, we show that Ω attracts all solutions of the model (3.9) initiating in $\mathbb{R}^3_+$. By Lemma 2.2, $\lim_{t\to\infty} E_\alpha(-\mu^\alpha t^\alpha) = 0$. From (4.5), we see that $\lim_{t\to\infty} N(t) = \frac{\Lambda^\alpha}{\mu^\alpha}$. Hence, Ω attracts all solutions of the model (3.9) initiating in $\mathbb{R}^3_+$. This completes the proof of the theorem. □

5. Equilibria and stability analysis

5.1. Stability of user-free equilibrium

It is clear that the model (3.9) has a unique user-free equilibrium (which is equivalent to the disease-free equilibrium in epidemiological models)

$$E_0 = \left(\frac{\Lambda^\alpha}{\mu^\alpha}, 0, 0\right). \tag{5.1}$$

We evaluate the associated Jacobian of this model at E_0, which takes the form

$$J = \begin{pmatrix} -\beta^\alpha I - \mu^\alpha & -\beta^\alpha S & 0 \\ \beta^\alpha I & \beta^\alpha S - \gamma^\alpha R - (\mu^\alpha + \nu^\alpha) & -\gamma^\alpha I \\ 0 & \gamma^\alpha R + \nu^\alpha & \gamma^\alpha I - \mu^\alpha \end{pmatrix}. \tag{5.2}$$

At E_0, the Jacobian

$$J(E_0) = \begin{pmatrix} -\mu^\alpha & -\frac{\beta^\alpha \Lambda^\alpha}{\mu^\alpha} & 0 \\ 0 & \frac{\beta^\alpha \Lambda^\alpha}{\mu^\alpha} - (\mu^\alpha + \nu^\alpha) & 0 \\ 0 & \nu^\alpha & -\mu^\alpha \end{pmatrix}$$

has the eigenvalues

$$\lambda_1 = \lambda_2 = -\mu^\alpha \quad \text{and} \quad \lambda_3 = \frac{\beta^\alpha \Lambda^\alpha}{\mu^\alpha} - (\mu^\alpha + \nu^\alpha).$$

The eigenvalues λ_1 and λ_2 are obviously negative, and λ_3 is negative if and only if

$$R_0^\alpha := \frac{\beta^\alpha \Lambda^\alpha}{\mu^\alpha(\mu^\alpha + \nu^\alpha)} < 1. \tag{5.3}$$

The scalar R_0^α is a dimensionless threshold quantity. When $\alpha = 1$, R_0^α is usually referred to as the reproduction number of the network, which measures the number of new secondary OSN users one infectious OSN user will produce in a population consisting only of potential OSN users.

From the above analysis and Lemma 2.3, the following result is immediate.

Theorem 5.1. *The user-free equilibrium E_0 is locally asymptotically stable if $R_0^\alpha < 1$ and unstable if $R_0^\alpha > 1$.*

Theorem 5.1 shows that if the initial values $(S_0, I_0, R_0) \in \mathbb{R}^3_+$ are sufficiently close to E_0, the unique solution of the model (3.9), with the ICs (3.4), converges to E_0. However, no explicit region of attraction is given here. By using the Lyapunov function method, we next obtain an explicit region of attraction.

Theorem 5.2. *Assume that $R_0^\alpha < 1$. The compact set Ω, defined by (4.1), is a region of attraction of the user-free equilibrium E_0.*

Proof. We need to show that, for every $(S_0, I_0, R_0) \in \Omega$, the unique solution (S, I, R) of the model (3.9), with the ICs (3.4), converges to E_0. Define the Lyapunov function $V_0(t)$ by

$$V_0(t) = \frac{1}{2} I^2 + \frac{1}{2}\left(S - \frac{\Lambda^\alpha}{\mu^\alpha} + I + R\right)^2.$$

By Theorem 4.1, the set Ω is positively invariant. Since $(S_0, I_0, R_0) \in \Omega$, we have $S \le \frac{\Lambda^\alpha}{\mu^\alpha}$. From Lemma 2.4(a) and (3.9), it follows that

$$\begin{aligned}
{}_0^C D_t^\alpha V_0(t) &\le I({}_0^C D_t^\alpha I) + \left(S - \frac{\Lambda^\alpha}{\mu^\alpha} + I + R\right) {}_0^C D_t^\alpha \left(S - \frac{\Lambda^\alpha}{\mu^\alpha} + I + R\right) \\
&= I[\beta^\alpha S I - \gamma^\alpha I R - (\mu^\alpha + \nu^\alpha) I] + \left(S - \frac{\Lambda^\alpha}{\mu^\alpha} + I + R\right)\left[\Lambda^\alpha - \mu^\alpha(S + I + R)\right] \\
&\le I^2 \left(\frac{\beta^\alpha \Lambda^\alpha}{\mu^\alpha} - (\mu^\alpha + \nu^\alpha)\right) - \gamma^\alpha I^2 R - \mu^\alpha \left(S - \frac{\Lambda^\alpha}{\mu^\alpha} + I + R\right)^2 \\
&= (\mu^\alpha + \nu^\alpha) I^2 \left(\frac{\beta^\alpha \Lambda^\alpha}{\mu^\alpha(\mu^\alpha + \nu^\alpha)} - 1\right) - \gamma^\alpha I^2 R - \mu^\alpha \left(S - \frac{\Lambda^\alpha}{\mu^\alpha} + I + R\right)^2 \\
&= (\mu^\alpha + \nu^\alpha) I^2 \left(R_0^\alpha - 1\right) - \gamma^\alpha I^2 R - \mu^\alpha \left(S - \frac{\Lambda^\alpha}{\mu^\alpha} + I + R\right)^2.
\end{aligned}$$

Since $R_0^\alpha < 1$, we have ${}_0^C D_t^\alpha V_0(t) \le 0$. Moreover, ${}_0^C D_t^\alpha V_0(t) = 0$ if and only if $S + R = \frac{\Lambda^\alpha}{\mu^\alpha}$ and $I = 0$; i.e.,

$$E = \{(S, I, R) \ : \ {}_0^C D_t^\alpha V_0(t) = 0\} = \left\{(S, 0, R) \ : \ S + R = \frac{\Lambda^\alpha}{\mu^\alpha}\right\}.$$

By Lemma 2.5, every solution of model (3.9) initiating in Ω tend to the largest invariant set in E. Thus, $\lim_{t\to\infty} I(t) = 0$. For $I = 0$, from (3.9) we obtain

$$\begin{cases} {}_0^C D_t^\alpha S = \Lambda^\alpha - \mu^\alpha S, \\ {}_0^C D_t^\alpha R = -\mu^\alpha R. \end{cases} \tag{5.4}$$

In a manner similar to obtaining (4.5), we find that the solution of (5.4) is

$$\begin{cases} S(t) = \left(-\frac{\Lambda^\alpha}{\mu^\alpha} + S(0)\right) E_\alpha(-\mu^\alpha t^\alpha) + \frac{\Lambda^\alpha}{\mu^\alpha}, \\ R(t) = R(0) E_\alpha(-\mu^\alpha t^\alpha). \end{cases}$$

By Lemma 2.2, $\lim_{t\to\infty} S(t) = \frac{\Lambda^\alpha}{\mu^\alpha}$ and $\lim_{t\to\infty} R(t) = 0$. Thus, $(S, I, R) \to E_0$ as $t \to \infty$. This completes the proof of the theorem. □

5.2. Stability of user-prevailing equilibrium

We first show the existence of a unique user-prevailing equilibrium of the model (3.9) if $R_0^\alpha > 1$. Here the user-prevailing equilibrium is the analogue of the endemic equilibrium in epidemiological models.

Theorem 5.3. *Assume that $R_0^\alpha > 1$. The model (3.9) has a unique user-prevailing equilibrium $E^* = (S^*, I^*, R^*)$, where*

$$S^* = \frac{\Lambda^\alpha}{\beta^\alpha I^* + \mu^\alpha}, \quad I^* = \frac{\mu^\alpha R^*}{\gamma^\alpha R^* + \nu^\alpha}, \tag{5.5}$$

and R^* is the unique positive solution of the quadratic equation in R given by

$$\begin{aligned} &\mu^\alpha(\beta^\alpha + \gamma^\alpha)\gamma^\alpha R^2 + [(\beta^\alpha + \gamma^\alpha)\mu^\alpha(\mu^\alpha + \nu^\alpha) \\ &\qquad + (\mu^\alpha \nu^\alpha - \beta^\alpha \Lambda^\alpha)\gamma^\alpha] R + \beta^\alpha \Lambda^\alpha \nu^\alpha \left(\frac{1}{R_0^\alpha} - 1\right) = 0. \end{aligned} \tag{5.6}$$

Remark 5.1. Since $R_0^\alpha > 1$, (5.6) has a negative constant term and a positive discriminant. Thus, it has a unique positive solution R^*.

Proof. From Definition 2.4, a user-prevailing equilibrium of the model (3.9) satisfies the equations

$$\begin{cases} 0 = \Lambda^\alpha - \beta^\alpha S I - \mu^\alpha S, \\ 0 = \beta^\alpha S I - \gamma^\alpha I R - (\mu^\alpha + \nu^\alpha) I, \\ 0 = \gamma^\alpha I R + \nu^\alpha I - \mu^\alpha R. \end{cases} \tag{5.7}$$

Using the first and the equations in (5.7), we have

$$S=\frac{\Lambda^\alpha}{\beta^\alpha I+\mu^\alpha}\quad\text{and}\quad I=\frac{\mu^\alpha R}{\gamma^\alpha R+\nu^\alpha},\tag{5.8}$$

from which

$$S=\frac{\Lambda^\alpha}{\frac{\beta^\alpha\mu^\alpha R}{\gamma^\alpha R+\nu^\alpha}+\mu^\alpha}=\frac{(\gamma^\alpha R+\nu^\alpha)\Lambda^\alpha}{\mu^\alpha(\beta^\alpha+\gamma^\alpha)R+\mu^\alpha\nu^\alpha}.\tag{5.9}$$

Adding the last two equations in (5.7) yields

$$\beta^\alpha SI-\mu^\alpha I=\mu^\alpha R.\tag{5.10}$$

We use (5.8) and (5.9) to eliminate S and I and obtain

$$\frac{\beta^\alpha(\gamma^\alpha R+\nu^\alpha)\Lambda^\alpha\mu^\alpha R}{[\mu^\alpha(\beta^\alpha+\gamma^\alpha)R+\mu^\alpha\nu^\alpha](\gamma^\alpha R+\nu^\alpha)}-\frac{\mu^{2\alpha}R}{\gamma^\alpha R+\nu^\alpha}=\mu^\alpha R.$$

Since we are looking for user-prevailing equilibria, $I\neq 0$. By the second equation in (5.8), $R\neq 0$. Thus, we can divide the above equation by $\mu^\alpha R$ to obtain

$$\frac{\beta^\alpha(\gamma^\alpha R+\nu^\alpha)\Lambda^\alpha}{[\mu^\alpha(\beta^\alpha+\gamma^\alpha)R+\mu^\alpha\nu^\alpha](\gamma^\alpha R+\nu^\alpha)}-\frac{\mu^\alpha}{\gamma^\alpha R+\nu^\alpha}=1,$$

and (5.6) follows. By Remark 5.1, (5.6) has a unique positive solution R^*. Once R^* is known, we can use the second equation in (5.8) to get a positive I^* and the first equation in (5.8) to obtain a positive S^*; i.e., we have (5.5). This completes the proof of the theorem. □

Remark 5.2. We present an alternative way to show the existence of the unique user-prevailing equilibrium $E^*=(S^*,I^*,R^*)$ of (3.9). As in the proof of Theorem 5.1, a user-prevailing equilibrium of (3.9) satisfies (5.7). Moreover, (5.8) and (5.10) hold. Using the third equation in (5.7), we have

$$R=\frac{\nu^\alpha I}{\mu^\alpha-\gamma^\alpha I}.\tag{5.11}$$

From (5.11), we see that $0\le I\le\frac{\mu^\alpha}{\gamma^\alpha}$. This is because R will be negative if $I>\frac{\mu^\alpha}{\gamma^\alpha}$. Substituting the first equation in (5.8) and (5.11) into (5.10), we obtain

$$\frac{\beta^\alpha\Lambda^\alpha I}{\beta^\alpha I+\mu^\alpha}-\mu^\alpha I=\frac{\mu^\alpha\nu^\alpha I}{\mu^\alpha-\gamma^\alpha I}.$$

As we are searching for user-prevailing equilibria, $I\neq 0$. Then dividing the above equation by I yields

$$\frac{\beta^\alpha\Lambda^\alpha}{\beta^\alpha I+\mu^\alpha}-\mu^\alpha=\frac{\mu^\alpha\nu^\alpha}{\mu^\alpha-\gamma^\alpha I}.\tag{5.12}$$

Motivated by (5.12), we introduce the function f defined by

$$f(I)=\frac{\beta^\alpha\Lambda^\alpha}{\beta^\alpha I+\mu^\alpha}-\frac{\mu^\alpha\nu^\alpha}{\mu^\alpha-\gamma^\alpha I}-\mu^\alpha.$$

Then $f(I)\to-\infty$ as $I\to\left(\frac{\mu^\alpha}{\gamma^\alpha}\right)^-$,

$$f(0)=\frac{\beta^\alpha\Lambda^\alpha}{\mu^\alpha}-\mu^\alpha-\nu^\alpha=\frac{\beta^\alpha\Lambda^\alpha-\mu^\alpha(\mu^\alpha+\nu^\alpha)}{\mu^\alpha}>0\quad\text{if } R_0^\alpha>1,$$

and

$$f'(I)=-\frac{\beta^{2\alpha}\Lambda^\alpha}{(\beta^\alpha I+\mu^\alpha)^2}-\frac{\mu^\alpha\nu^\alpha\gamma^\alpha}{(\mu^\alpha-\gamma^\alpha I)^2}<0\quad\text{for } 0\le I<\frac{\mu^\alpha}{\gamma^\alpha}.$$

Thus, there exists a unique $I^*\in\left(0,\frac{\mu^\alpha}{\gamma^\alpha}\right)$ such that $f(I^*)=0$; i.e., (5.12) has a unique positive solution I^*. Using the first equation in (5.8) and (5.11), we can compute S^* and R^*.

We now study the stability of the user-prevailing equilibrium $E^* = (S^*, I^*, R^*)$.

Theorem 5.4. *The user-prevailing equilibrium $E^* = (S^*, I^*, R^*)$ is globally asymptotically stable.*

Proof. Let $\Phi(x) = x - 1 - \ln x$, $x > 0$. Define the Lyapunov function $V_1(t)$ by

$$V_1(t) = F_1(t) + F_2(t) + F_3(t) + F_4(t),$$

where

$$F_1(t) = S^* \Phi\left(\frac{S}{S^*}\right), \quad F_2(t) = I^* \Phi\left(\frac{I}{I^*}\right), \quad F_3(t) = \frac{\gamma^\alpha (R^*)^2}{\gamma^\alpha R^* + \nu^\alpha} \Phi\left(\frac{R}{R^*}\right),$$

and

$$F_4(t) = \left(S^* + I^* + R^*\right) \Phi\left(\frac{S + I + R}{S^* + I^* + R^*}\right).$$

Below, we evaluate the α-th order Caputo derivatives of F_i, $i = 1, 2, 3, 4$, by applying Lemma 2.4(b). From the first equation in (5.7), we have

$$\Lambda^\alpha = \beta^\alpha S^* I^* + \mu^\alpha S^*.$$

Using this and the first equation in (3.9), we obtain

$$\begin{aligned}
{}_0^C D_t^\alpha F_1(t) &\le \frac{S - S^*}{S} {}_0^C D_t^\alpha S \\
&= \frac{S - S^*}{S} (\Lambda^\alpha - \beta^\alpha S I - \mu^\alpha S) \\
&= \frac{S - S^*}{S} \left[\mu^\alpha (S^* - S) + \beta^\alpha (S^* I^* - S I)\right] \\
&= \frac{S - S^*}{S} \left[\mu^\alpha (S^* - S) + \beta^\alpha I^* (S^* - S) + \beta^\alpha S (I^* - I)\right] \\
&= -\frac{(\mu^\alpha + \beta^\alpha I^*)(S - S^*)^2}{S} + \beta^\alpha (S - S^*)(I^* - I).
\end{aligned} \tag{5.13}$$

In view of the second equation in (5.7), we have

$$\mu^\alpha + \nu^\alpha = \beta^\alpha S^* - \gamma^\alpha R^*.$$

By the second equation in (3.9), we obtain

$$\begin{aligned}
{}_0^C D_t^\alpha F_2(t) &\le \frac{I - I^*}{I} {}_0^C D_t^\alpha I \\
&= \frac{I - I^*}{I} [\beta^\alpha S I - \gamma^\alpha I R - (\mu^\alpha + \nu^\alpha) I] \\
&= \frac{I - I^*}{I} [\beta^\alpha S I - \gamma^\alpha I R - (\beta^\alpha S^* - \gamma^\alpha R^*) I] \\
&= \frac{I - I^*}{I} [\beta^\alpha I (S - S^*) - \gamma^\alpha I (R - R^*)] \\
&= \beta^\alpha (S - S^*)(I - I^*) - \gamma^\alpha (I - I^*)(R - R^*).
\end{aligned} \tag{5.14}$$

From the third equation in (5.7), we see that

$$\mu^\alpha = \gamma^\alpha I^* + \frac{\nu^\alpha I^*}{R^*}.$$

This, together with the third equation in (3.9), implies that

$$\begin{aligned}
{}_0^C D_t^\alpha F_3(t) &\le \frac{\gamma^\alpha R^*}{\gamma^\alpha R^* + \nu^\alpha} \frac{R - R^*}{R} {}_0^C D_t^\alpha R \\
&= \frac{\gamma^\alpha R^*}{\gamma^\alpha R^* + \nu^\alpha} \frac{R - R^*}{R} (\gamma^\alpha I R + \nu^\alpha I - \mu^\alpha R)
\end{aligned}$$

$$
\begin{aligned}
&= \frac{\gamma^\alpha R^*}{\gamma^\alpha R^* + \nu^\alpha} \frac{R - R^*}{R} \left(\gamma^\alpha I R + \nu^\alpha I - \gamma^\alpha I^* R - \frac{\nu^\alpha I^* R}{R^*} \right) \\
&= \frac{\gamma^\alpha R^*}{\gamma^\alpha R^* + \nu^\alpha} \frac{R - R^*}{R} \left[\gamma^\alpha R (I - I^*) + \nu^\alpha R \left(\frac{I}{R} - \frac{I^*}{R^*} \right) \right] \\
&= \frac{\gamma^\alpha R^* (R - R^*)}{\gamma^\alpha R^* + \nu^\alpha} \left\{ \gamma^\alpha (I - I^*) + \frac{\nu^\alpha [I(R^* - R) + R(I - I^*)]}{R R^*} \right\} \\
&= \gamma^\alpha (I - I^*)(R - R^*) - \frac{\gamma^\alpha \nu^\alpha I (R - R^*)^2}{(\gamma^\alpha R^* + \nu^\alpha) R}. \qquad (5.15)
\end{aligned}
$$

Adding the equations in (5.7) together yields

$$\Lambda^\alpha = \mu^\alpha (S^* + I^* + R^*).$$

Using this equation and (3.9), we obtain

$$
\begin{aligned}
{}_0^C D_t^\alpha F_4(t) &\le \frac{S + I + R - (S^* + I^* + R^*)}{S + I + R} {}_0^C D_t^\alpha (S + I + R) \\
&= \frac{(S - S^*) + (I - I^*) + (R - R^*)}{S + I + R} [\Lambda^\alpha - \mu^\alpha (S + I + R)] \\
&= \frac{(S - S^*) + (I - I^*) + (R - R^*)}{S + I + R} \times \\
&\qquad \mu^\alpha [(S^* - S) + (I^* - I) + (R^* - R)] \\
&= -\frac{\mu^\alpha [(S - S^*) + (I - I^*) + (R - R^*)]^2}{S + I + R}. \qquad (5.16)
\end{aligned}
$$

From (5.13)–(5.16), it follows that

$$
\begin{aligned}
{}_0^C D_t^\alpha V_1(t) &\le {}_0^C D_t^\alpha F_1(t) + {}_0^C D_t^\alpha F_2(t) + {}_0^C D_t^\alpha F_3(t) + {}_0^C D_t^\alpha F_4(t) \\
&= -\frac{(\mu^\alpha + \beta^\alpha I^*)(S - S^*)^2}{S} - \frac{\gamma^\alpha \nu^\alpha I (R - R^*)^2}{(\gamma^\alpha R^* + \nu^\alpha) R} \\
&\quad - \frac{\mu^\alpha [(S - S^*) + (I - I^*) + (R - R^*)]^2}{S + I + R}.
\end{aligned}
$$

Thus, ${}_0^C D_t^\alpha V_1(t) \le 0$ and ${}_0^C D_t^\alpha V_1(t) = 0$ if and only if $S = S^*$, $I = I^*$, and $R = R^*$. So the largest invariant set of $\{(S, I, R) : {}_0^C D_t^\alpha V_1(t) = 0\}$ is the singleton $\{E^*\}$. From Theorem 4.1, we note that the set Ω attracts all solutions of model (3.9) initiating in $\mathbb{R}^3_+$ By Lemma 2.5, E^* is global asymptotically stable. This completes the proof of the theorem. □

Remark 5.3. From (5.3), we see that the threshold quantity R_0^α does not depend on the infectious abandonment rate γ. The analysis in this section shows that γ has no contribution to the stability of E_0 and E^*. However, γ has an affect the location of E^* in $\mathbb{R}^3_+$. This is evident in Theorem 5.3 and the simulations in the next section.

6. Numerical simulations

An Adams-type predictor–corrector method [13,14,18] is applied to obtain a numerical solution of the model (3.9). The reader is referred to [13] for the details of the algorithm. The values of the parameters in the model (3.9) and the initial values are chosen for illustration purposes.

6.1. User-free equilibrium

We first consider the user-free equilibrium E_0 for model (3.9) with the parameters given in Table 3.

From (5.1) and (5.3), it follows that $E_0 \simeq (0.1395, 0, 0)$ and $R_0^\alpha < 1$. By Theorem 5.1, E_0 is locally asymptotically stable. In view of Theorem 5.2, the numerical simulations are carried out using initial points from Ω defined by (4.1). The initial points are given in Table 4. The trajectories are shown in Fig. 2. The numerical simulations show that all the trajectories converge to E_0. This is consistent with Theorems 5.1 and 5.2.

Table 3
Parameters for the user-free equilibrium E_0.

Parameter	Value	Parameter	Value
α	0.6	β	0.1
γ	0.03	Λ	0.03
μ	0.8	ν	0.4

Table 4
List of initial points (S_0, I_0, R_0).

No.	S_0	I_0	R_0
1	0.0002	0.0022	0.0019
2	0.1302	0.0022	0.0019
3	0.0002	0.0205	0.0019
4	0.1302	0.0205	0.0019
5	0.0002	0.0022	0.0131
6	0.1302	0.0022	0.0131
7	0.0002	0.0205	0.0131
8	0.1302	0.0205	0.0131

Table 5
Parameters for the endemic equilibrium E^*.

Parameter	Value	Parameter	Value
α	0.6	β	0.1
γ	0.03	Λ	0.07
μ	0.008	ν	0.4

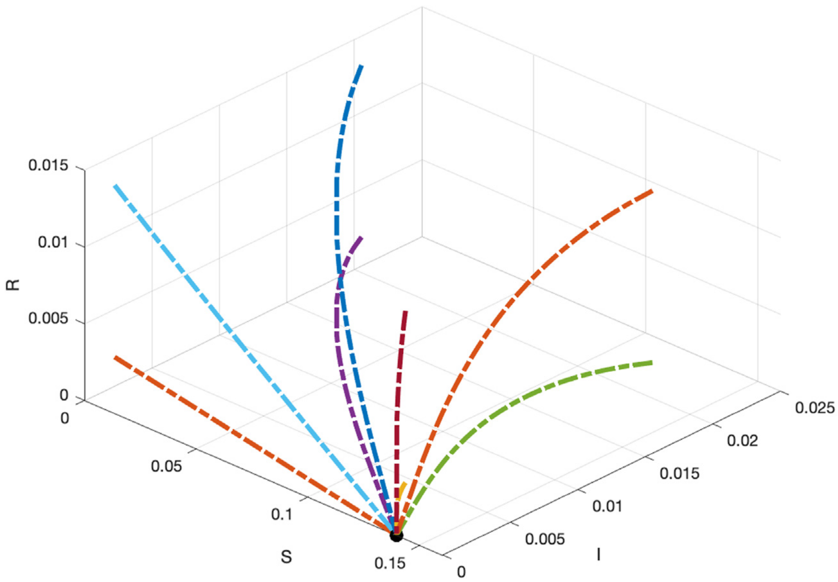

Fig. 2. Locally asymptotically stability of E_0.

6.2. User-prevailing equilibrium

We now consider the model (3.9) with the parameters indicated in Table 5. From (5.3)–(5.6), $E^* \simeq (2.8755, 0.0611, 0.7380)$ and $R_0^\alpha > 1$. By Theorem 5.4, E^* is globally asymptotically stable. The numerical simulations are

Table 6
List of initial points (S_0, I_0, R_0).

No.	S_0	I_0	R_0
1	0.8	1	0.7
2	4	1	0.7
3	0.8	3	0.7
4	4	3	0.7
5	0.8	1	1.5
6	4	1	1.5
7	0.8	3	1.5
8	4	3	1.5

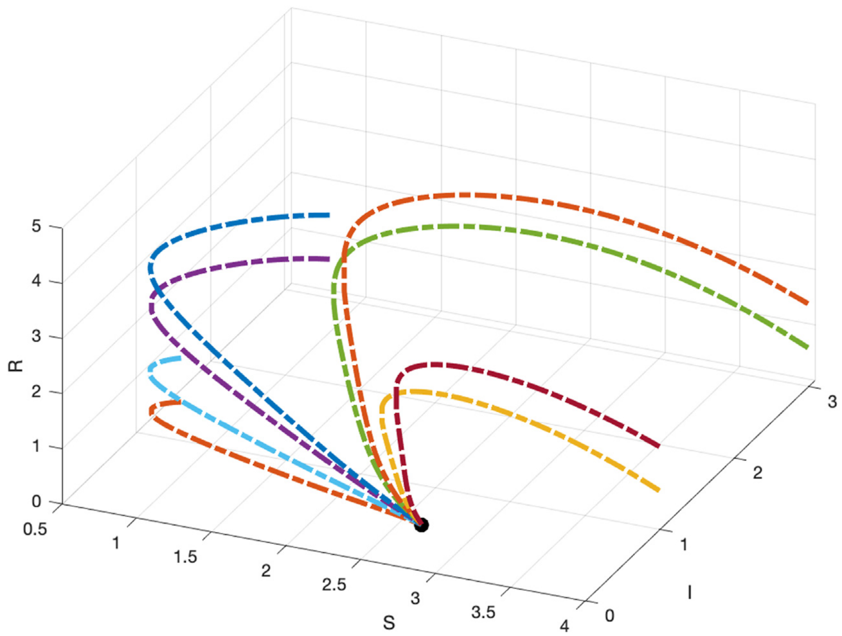

Fig. 3. Globally asymptotically stability of E^*.

carried out based on the initial points indicated in Table 6. The trajectories are shown in Fig. 3. The numerical simulations show that all the trajectories converge to E^*. This is consistent with Theorem 5.4.

6.3. Dependence of parameters

We next investigate the impact of the parameters γ and α on the solution while all other parameters are fixed.

6.3.1. Dependence on γ

In view of (5.3), it is notable that R_0^α is independent of the noninfectious abandonment rate γ. However, as indicated above, γ will impact the location of the user-prevailing equilibrium E^* given by (5.5) and (5.6). To illustrate this, the locations of E^* with respect to various values of γ, while other parameters are fixed as in Table 5, are given in Fig. 4.

6.3.2. Dependence on α

Finally, we investigate the impact of index of memory α to the solution while other parameters are fixed. The values of β, γ, Λ, μ, and ν are given as in Table 5. The initial point is $(0.8, 1, 0.7)$. The numerical simulations are carried out for $\alpha = 0.4, 0.6, 0.8, 0.9, 0.95$, and 1. When $\alpha = 1$, the model (3.9) reduces to the first-order

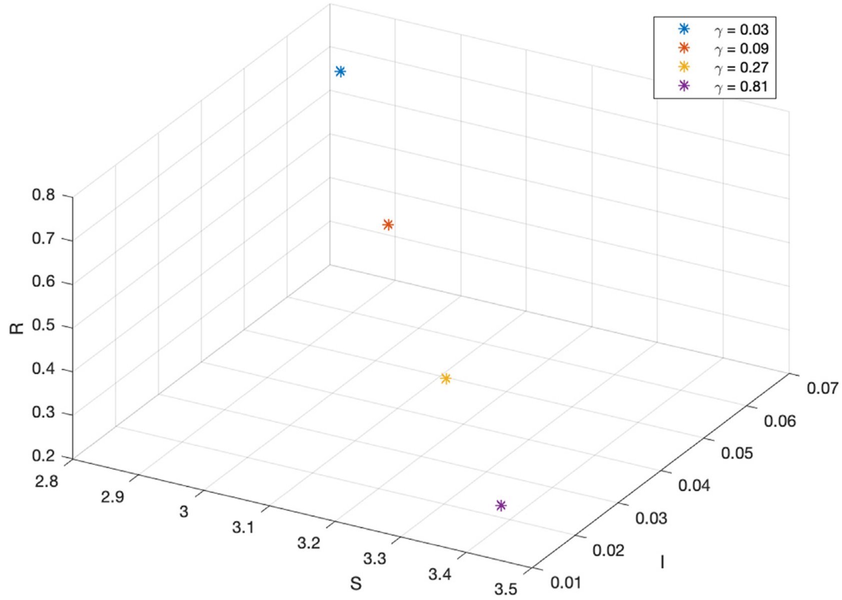

Fig. 4. Location of E^* with respect to γ.

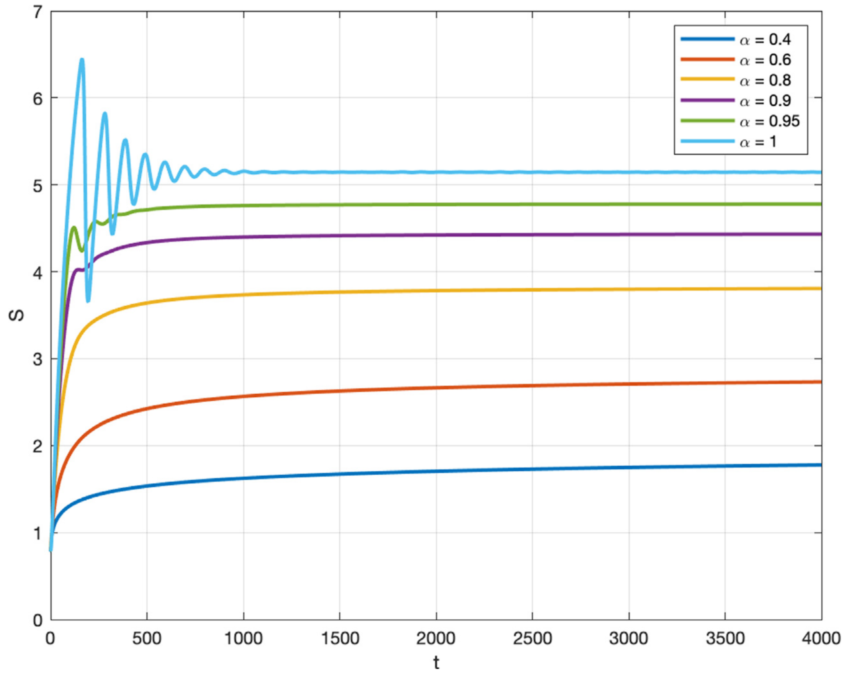

Fig. 5. Graph of S with respect to α.

ODE system (3.2). The solutions, S, I, R, are plotted in Figs. 5–7, respectively. The trajectories are plotted in Fig. 8. These figures suggest that the dynamical behavior of the model (3.9) varies with respect to α and that different types of dynamical behaviors may be obtained by simply adjusting the value of α. This illustrates that fractional differential equation models offer more degrees of freedom than the traditional integer order models and thus modeling with fractional differential equations has more advantages than using the traditional integer order models.

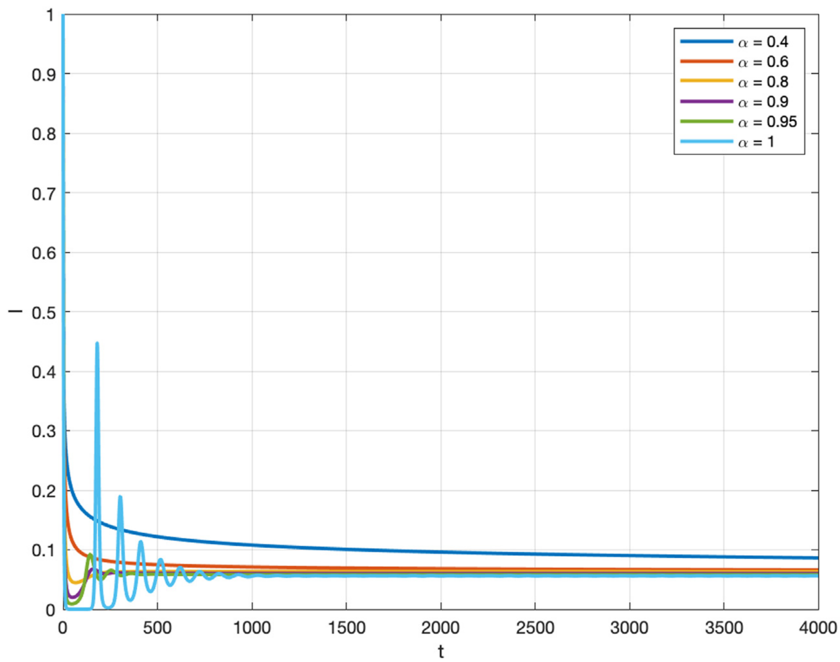

Fig. 6. Graph of I with respect to α.

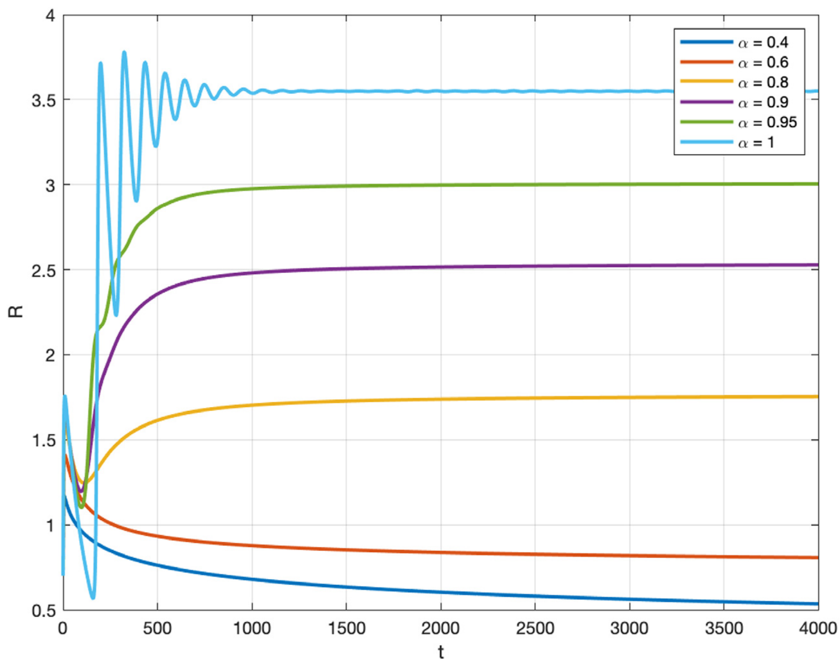

Fig. 7. Graph of R with respect to α.

7. Case study: Fitting model to instagram data

In this section, we demonstrate the performance of model (3.9) by fitting it to the historical Instagram user data given in [40]. Let $\{\hat{I}(t_0), \hat{I}(t_1), \ldots, \hat{I}(t_K)\}$ represent the active Instagram users (observations) at times $t_0, \ldots, t_K$.

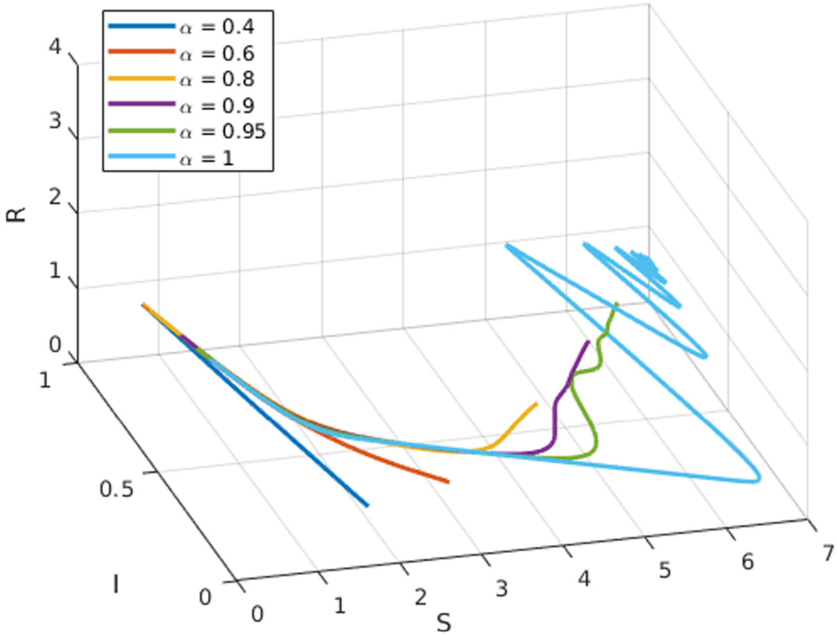

Fig. 8. Trajectories of the model (3.9) with respect to α.

Table 7
Model fitting parameters.

Parameter	Value	Parameter	Value
α	0.3359	β	$1.8024e{-}4$
γ	$5.2713e{-}4$	Λ	0.9812
μ	$1.1164e{-}5$	ν	$3.1131e{-}12$

Then the model parameters $\Theta := \{\Lambda, \alpha, \beta, \gamma, \mu, \nu\}$ are determined by minimizing

$$L(\Theta) = \sum_{i=0}^{K} \omega_i \left(I(t_i; \Theta) - \hat{I}(t_i) \right)^2,$$

where $\omega_0, \ldots, \omega_K$ are pre-set weights and $I(t; \Theta)$ denotes the solution I in model (3.9) subject to parameter set Θ. Due to the fact that it is difficult to get real data for S and R, we simply let $R_0 = 0$ and S_0 be the total internet users at t_0.

A total of 12 observations of the monthly active Instagram users between January 2013 and June 2018 are given in [40]. The first 10 observations are used for parameter estimation. The parameter values are given in Table 7. Then with these values, the model is used to predict the last two observations. The predicted values and the historical data are given in Fig. 9. It is clear that the predicted values matches the real data very well.

8. Conclusion

The preceding discussion illustrates how fractional derivatives can be applied to the study of the OSN dynamics. We have discussed the fractional-order SIR model (3.9), as a generalization of the traditional SIR model with demography, to understand the user adoption and abandonment of OSNs. This model employs the Caputo fractional derivative and incorporates infectious and noninfectious abandonment dynamics. We have established the existence and uniqueness of nonnegative solutions and investigated the existence and stability of the model's equilibria, with the latter being achieved using the Jacobian matrix technique and the Lyapunov function method. More precisely, when the threshold quantity R_0^α satisfies $R_0^\alpha < 1$, the user-free equilibrium E_0 is locally asymptotically stable. This asserts that all the users will eventually lose interest in the OSN. Likewise, when $R_0^\alpha > 1$, the user-prevailing

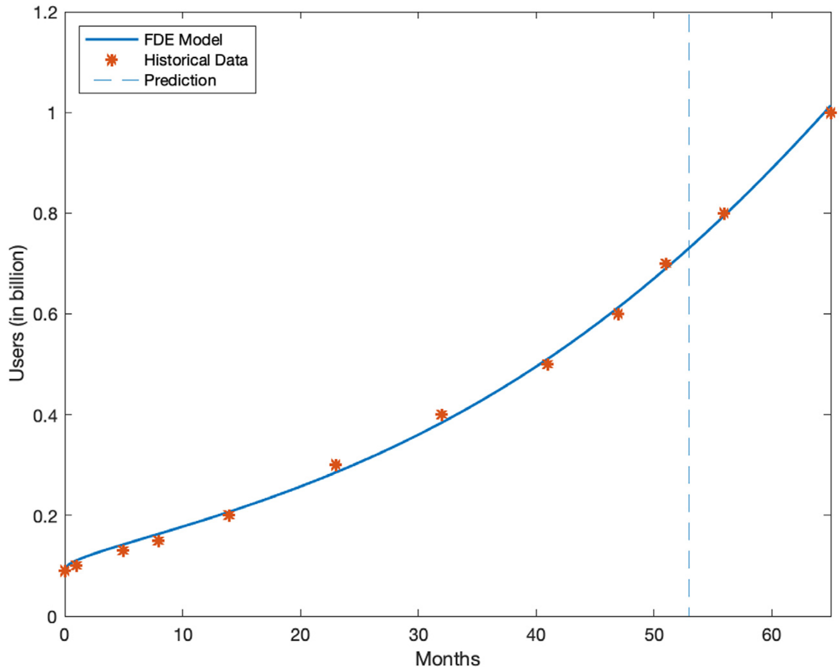

Fig. 9. Model fitting for Instagram users from 2013–2018. The observations on the left-hand side of the dash line are used for model fitting.

equilibrium E^* exists and is globally asymptotically stable. This means that the OSN always attracts the users' interest and that the users will largely prevail. Thus, the OSN providers may use R_0^α to obtain some useful information to gauge the performance of their networks. By (5.3), we see that R_0^α is increasing in the transmission rate β and the migration rate Λ, and decreasing in the natural death rate μ and the noninfectious abandonment rate ν. An OSN provider can influence the values of β, Λ, and ν by taking necessary marketing strategies such as TV advertisements and email marketing to increase people's awareness of the network. This will very possibly increase the values of β and Λ, and decrease the value of ν, and consequently, the value of R_0^α will be increased. Moreover, as illustrated in Section 7, our model can be used to predict the future users of an OSN.

In view of (5.3), it is interesting that R_0^α depends on all the parameters in the model except the infectious abandonment rate γ, which is not what one would expect. Our main results show that γ does not affect the stability of E_0 and E^*. However, γ does alter where E^* is positioned in R_+^3, as is evident in (5.5) and (5.6). Our numerical simulations, based on a variation of the Adams-type predictor–corrector method, confirm what we observe theoretically. In fact, these simulations also show that the order α of the model influences the dynamics of the S, I, R curves and the trajectories of the model.

Acknowledgments

During the preparation of this work, J.R. Graef, L. Kong, and A. Ledoan received support from the University of Tennessee at Chattanooga's SimCenter CEACSE (Center of Excellence in Applied Computational Science and Engineering) Grants Program, and M. Wang received support from the National Science Foundation Grant No. 1830489.

References

[1] N. Aguila-Camacho, M.A. Duarte-Mermoud, J.A. Gallegos, Lyapunov Functions for fractional order systems, Commun. Nonlinear Sci. Numer. Simul. 19 (2014) 2951–2957.

[2] C.N. Angstmann, B.I. Henry, A.V. McGann, A fractional-order infectivity and recovery model, Fractal Fract. 1 (2017) 1–11.

[3] K. Baisad, S. Moonchai, Analysis of stability and Hopf bifurcation in a fractional Gauss-type predator–prey model with Allee effect and holling type-III functional response, Adv. Difference Equ. 2018 (82) (2018) 20.

[4] D. Baleanu, K. Diethelm, E. Scals, J. J, Trujillo Fractional Calculus: Models and Numerical Methods, World Scientific, Singapore, 2012.
[5] D.J. Bartholomew, Recent developments in nonlinear stochastic modelling of social processes, Canadian J. Stat. 12 (1984) 39–52.
[6] F. Benevenuto T. Rodrihues, M. Cha, V. Almeida, Characterizing user behavior in online social networks, in: Proceedings of ACM SIGCOMMM International Measurement Conference, 2009.
[7] L.M. Bettencourt, A. Cintrn-Arias, D.I. Kaiser, C. Castillo-Chvez, The power of a good idea: quantitative modeling of the spread of ideas from epidemiological models, Physica A 364 (2006) 513–536.
[8] J. Cannarella, J.A. Spencer, Epidemiological modeling of online social network dynamics, 17 January, 2014, arXiv:1401.4208v1.
[9] G. Dai, R. Ma, H. Wang, F. Wang, K. Xu, Partial differential equations with Robin boundary conditions in online social networks, Discrete Contin. Dyn. Syst. Ser. B 20 (2015) 1609–1624.
[10] S. Das, P.K. Gupta, A mathematical model on fractional Lotka–Volterra equations, J. Theoret. Biol. 277 (2011) 1–6.
[11] K. Diethelm, The Analysis of Fractional Differential Equations, Springer, Berlin, 2010.
[12] K. Diethelm, A fractional calculus based model for the simulation of an outbreak of dengue fever, Nonlinear Dynam. 71 (2013) 613–619.
[13] K. Diethelm, N.J. Ford, A.D. Freed, A predictor–corrector approach for the numerical solution of fractional differential equations, Nonlinear Dynam. 29 (2002) 3–22.
[14] K. Diethelm, N.J. Ford, A.D. Freed, Detailed error analysis for a fractional Adams methods, Numer. Algorithms 36 (2004) 31–52.
[15] A. Dokoumetzidis, R. Magin, P. Macheras, A commentary on fractionalization of multi-compartmental models, J. Pharmacokinet Pharmacodyn. 37 (2010) 203–207.
[16] A. Dokoumetzidis, R. Magin, P. Macheras, Fractional kinetics in multi-compartmental systems, J. Pharmacokinet Pharmacodyn. 37 (2010) 507–524.
[17] M. Du, Z. Wang, H. Hu, Measuring memory with the order of fractional derivative, Sci. Rep. 3 (2013) 1–3.
[18] R. Garrappa, On linear stability of predictor–corrector algorithms for fractional differential equations, Internat. J. Comput. Math. 87 (2010) 2281–2290.
[19] R.K. Ghaziani, J. Alidousti, A.B. Eshkaftaki, Stability and dynamics of a fractional order Leslie–Gower prey–predator model, Appl. Math. Model. 40 (2016) 2075–2086.
[20] A. Guille, H. Hacis, C. Favre, D.A. Zighed, Information diffusion in online social networks, SIGMO Record 42 (2013) 17–28.
[21] E. Hanert, E. Schumacher, E. Deleersnijder, Front dynamics in fractional-order epidemic models, J. Theoret. Biol. 279 (2011) 9–16.
[22] A. Hughes, L. Palen, Twitter adoption and use in mass convergence and emergence events, Internat. J. Emergency Manag. 6 (2009) 248–260.
[23] L. Huo, X. Li, An interplay model for official information and rumor spreading with impulsive effects, Adv. Difference Equ. 2018 (164) (2019) 16.
[24] J. Huo, H. Zhao, L. Zhu, The effect of vaccines on backward bifurcation in a fractional order HIV model, Nonlinear Anal. RWA 26 (2015) 289–305.
[25] M. Javidi, N. Nyamoradi, Dynamic analysis of a fractional order prey-predator interaction with harvesting, Appl. Math. Model. 37 (2013) 8946–8956.
[26] J. Jiang, C. Wilson, X. Wang, P. Huang, W. Sha, Y. Dai, B. Zhao, Understanding latent interaction in online social networks, in: Proceedings of ACM SIGCOMMM International Measurement Conference, 2010.
[27] W. Kermack, A. McKendrick, A contribution to mathematical theory of epidemics, Proc. R. Soc. Lond. A 115 (1927) 700–721.
[28] A.A. Kilbas, H.M. Trujillo, J.J. Trujillo, Theory and Applications of Fractional Differential Equations, Boston, Elsevier, 2006.
[29] Q. Kong, A Short Course in Ordinary Differential Equations, Springer, New York, 2015.
[30] C. Lei, Z. Lin, H. Wang, The free boundary problem describing information diffusion in online social networks, J. Differential Equations 254 (2013) 1326–1341.
[31] K. Lerman, R. Ghosh, Information contagion: an empirical study of spread of news on digg and twitter social networks, in: Proceedings of International Conference on Weblogs and Social Media, ICWSM, 2010.
[32] J. Leskovec, M. Mcglohon, C. Faloutsos, N. Glance, M. Hurst, Cascading behavior in large blog graphs, in: SDM '07, 2007, pp. 551–556.
[33] Y. Li, Y. Chen, I. Podlubny, Stability of fractional-order nonlinear dynamic systems: Lyapunov direct method and generalized Mittag-Leffler stability, Comput. Math. Appl. 59 (2010) 1810–1823.
[34] W. Lin, Global existence theory and chaos control of fractional differential equations, J. Math. Anal. Appl. 332 (2007) 709–726.
[35] X. Liu, T. Li, X. Cheng, W. Liu, H. Xu, Spreading dynamics of a preferential information model with hesitation psychology on scale-free networks, Adv. Difference Equ. 2019 (279) (2019) 19pp.
[36] X. Liu, T. Li, M. Tian, Rumor spreading of a SEIR model in complex social networks with hesitating mechanism, Adv. Difference Equ. 2018 (391) (2018) 24pp.
[37] Y.F. Luchko, M. Rivero, J.J. Trujillo, M.P. Velasco, Fractional models, non-locality, and complex systems, Comput. Math. Appl. 59 (2010) 1048–1056.
[38] M. Martcheva, An Introduction To Mathematical Epidemiology, in: Texts in Applied Mathematics, vol. 61, Springer, London, 2015.
[39] A. Nazir, S. Raza, C.N. Chuah, Unveiling facebook: a measurement study of social network based applications, in: Proceedings of ACM SIGCOMMM International Measurement Conference, 2008.
[40] Number of monthly active Instagram users from January 2013 to June 2018, https://www.statista.com/statistics/253577/number-of-monthly-active-instagram-users/.
[41] I. Petras, Fractional-Order Nonlinear Systems: Modeling, Analysis and Simulation, Springer, London, 2011.

[42] C.M.A. Pinto, A.R.M. Carvalho, A latency fractional order model for HIV dynamics, J. Comput. Appl. Math. 312 (2017) 240–256.
[43] I. Podlubny, Fractional Differential Equations, Academic Press, New York, 1999.
[44] M. Saeedian, M. Khalighi, N. Azimi-Tafreshi, G.R. Jafari, M. Ausloos, Memory effects on epidemic evolution: the susceptible-infected-recovered epidemic model, Phys. Rev. E 95 (2) (2017) 022409, 9pp.
[45] T. Sardar, S. Rana, J. Chattopadhyay, A mathematical model of dengue transmission with memory, Commun. Nonlinear Sci. Numer. Simul. 22 (2015) 511–525.
[46] F. Schneider, A. Feldmann, B. Krishnamurthy, W. Willinger, Understanding online social network usage from a network perspective, in: Proceedings of ACM SIGCOMMM International Measurement Conference, 2009.
[47] G.V. Steeg, R. Ghosh, K. Lerman, What stops social epidemic? in: Proceedings of International AAAI Conference on Weblogs and Social Media, 2011.
[48] C. Vargas-De-León, Volterra-Type Lyapunov functions for fractional-order epidemic systems, Commun. Nonlinear Sci. Numer. Simul. 24 (2015) 75–85.
[49] T. Wang, J. He, X. Wang, An information spreading model based on online social networks, Physica A 490 (2018) 488–496.
[50] F. Wang, H. Wang, K. Xu, Diffusion logistic model towards predicting information diffusion in online social networks, in: 2012 32nd International Conference on Distributed Computing Systems Workshops, ICDCSW, 2012, pp. 133–139.
[51] D.J. Watts, A simple model of global cascades on random networks, Proc. Natl. Acad. Sci. 99 (2002) 5766–5771.
[52] J. Yang, J. Leskovec, Modeling information diffusion in implicit networks, in: SDM '10, 2010, pp. 599–608.